











Three New Chemical Constituents of *Dryopteris crassirhizoma* Nakai in Lianhua Qingwen Capsule and Investigation on Their Antiviral Potential Based on 3CL Hydrolase of SARS-CoV-2

Yunbo Sun ^{1,2#}, Tongxing Wang ^{2#}, Shuo Shen ^{3#}, Dan Bi ^{1,2},
Fengjun He ², Bin Hou ², Yifu Zhang ², Ya Tian ³,
Chuangfeng Zhang ^{1,2*} and Zhenhua Jia ^{2*}

¹Beijing Yiling Pharmaceutical Co., Ltd., Beijing 102600, P. R. China

²Hebei Academy of Integrated Traditional Chinese and Western Medicine,
Shijiazhuang, 050091, P. R. China

³Institute of Chinese Materia Medica, China Academy of Chinese Medical Sciences,
Beijing 100700, P. R. China

(Received January 17, 2023; Revised May 02, 2023; Accepted May 04, 2023)

Abstract: Three new chromone glycosides, named 2-methyl-5-hydroxyl-4-chromone-7-*O*- β -D-glucuronide (**1**), 2-ethyl-5-hydroxyl-4-chromone-7-*O*- β -D-glucuronide (**2**) and 1-acetyl-3-*C*- β -D-glucopyranosyl-5-methyl-phloroglucinyl-6-*O*- β -D-glucopyranoside (**6**), together with eight known compounds were isolated from the water extract of *Dryopteris crassirhizoma* Nakai, and the water extract preparation process is consistent with Lianhua Qingwen capsule. All the chemical structures of new compounds were characterized by 1D and 2D NMR spectra as well as high resolution mass and IR spectra. The chemical structures of known compounds were characterized by NMR spectra along with comparison of their spectroscopic data with those reported in the literature. The binding ability of these compounds to 3CL hydrolase of SARS-COV-2 was evaluated by molecular docking. The results showed that the chromone glycosides with glucuronic acid fragment had good docking effect with 3CL hydrolase and this indicated the chromone glucuronides could be further studied as potential antiviral compounds.

Keywords: *Dryopteris crassirhizoma* Nakai; chromone glycosides; molecular docking; molecular dynamics simulation. © 2023 ACG Publications. All rights reserved.

1. Introduction

Lianhua Qingwen Capsule (hereinafter referred to as LHQW) is a new Chinese patent medicine (SFDA Approval No.: Z20040063) developed under the guidance of collateral disease theory in traditional Chinese medicine for the treatment of cold and influenza, and it is composed of 13 Chinese

* Corresponding author: E-Mail: zcf4300@126.com (C. Zhang), jzhjiazhenhua@163.com (Z. Jia)
Phone: +86-13146651143

These authors contributed to this work equally.

A new iridoid from the wine-processed corni fructus

herbals. LHQW is the first new medicine approved through fast-track approval process by the National Medical Products Administration during the SARS epidemic and plays a pivotal role in the prevention and control of COVID-19 in China.

Dryopteris crassirhizoma Nakai, an important herb of LHQW, was first recorded in Shennong's Materia Medica, mainly distributed in Liaoning, Jilin and Heilongjiang of China [1-2]. Modern pharmacological research showed that *D. crassirhizoma* had antiviral, antitumor, anti-inflammatory and antioxidant activities [3-8]. In particular, its anti-influenza virus effect has received widespread attention, among which the herbal medicine and its chemical constituents of the influenza virus H5N1 neuraminidase inhibitory effect and the effect against the influenza A virus FM1 strain have been verified [9,10].

In order to clarify the pharmacodynamic material basis of *D. crassirhizoma*, a lot of phytochemical researches had been carried out. At present, resorcinols, flavonoids, terpenes, and phenylpropanoids had been isolated from the herbal medicine [6,9,11]. The above types of compounds were mostly isolated from its alcohol extract or organic extraction layer, and their polarities are relatively small; however, the *D. crassirhizoma* was extracted by water decocting method in the production process of LHQW. The polar ingredients could be extracted in large quantities during the decoction process, and this part of the ingredients was likely to have a greater impact on the efficacy. Therefore, in order to further explore the material basis of *D. crassirhizoma* in LHQW, and to find antiviral potential compounds, this paper conducted a systematic study on the chemical composition of its water extraction part, whose preparation process is consistent with LHQW.

At present, the novel coronavirus (SARS-CoV-2) is still raging around the world. As of 4 March 2022, the cumulative number of Corona Virus Disease 2019 (COVID-19) cases in the world is about 440 million, and the cumulative number of deaths is close to 6 million. Based on the application background of *D. crassirhizoma* in the field of anti-virus, the molecular docking technology was used to predict the effects of the isolated compounds on the 3CL hydrolase (Mpro) of SARS-CoV-2 [12,13]. 3CL hydrolase is used to hydrolyze the polyproteins pp1a and pp1ab of SARS-CoV-2 to produce nonstructural proteins involved in transcription and viral replication [12-14]. Therefore, 3CL hydrolase can be used as an important target to screen antiviral drugs. The related results of this paper provide a research basis for the development of SARS-CoV-2 drugs.

In the study, three new phenolic glycosides, 2-methyl-5-hydroxyl-4-chromone-7-*O*- β -D-glucuronide (**1**), 2-ethyl-5-hydroxyl-4-chromone-7-*O*- β -D-glucuronide (**2**) and 1-acetyl-3-*C*- β -D-glucopyranosyl-5-methyl-phlorogluciny-6-*O*- β -D-glucopyranoside (**6**), together with eight known compounds were isolated from the roots of *D. crassirhizoma* (Figure 1). Molecular docking results indicated that most of the compounds had antiviral potential, which could form a stable complex with 3CL hydrolase. The new findings in this study may provide some new hints for the design of antiviral drugs.

2. Materials and Methods

2.1. Apparatus and Reagents

IR spectra were recorded on an ALPHA FT-IR spectrometer (Bruker, Germany). NMR spectra were measured with either a AVANCE III HD 600 (600 MHz for ^1H NMR; 150 MHz for ^{13}C NMR) spectrometer (Bruker, Germany) or an NMR VNMRs 600 (600 MHz for ^1H NMR; 150 MHz for ^{13}C NMR) spectrometer (Agilent, USA) with tetramethylsilane (TMS) as internal reference and the chemical shifts were given in δ (ppm) and coupling constants in Hz. MS spectra were obtained on a Synapt G2-S mass spectrometer (Waters, USA) or Q-Exactive Orbitrap mass spectrometer (ThermoScientific, USA). Column chromatography was performed on AB-8 macroporous resin (Cangzhou Bon, China), 200-300 mesh column chromatography silica gel (Qingdao Ocean, China), Sephadex LH-20 (GE Healthcare, Germany), and RP-C18 (ODS-A, S-50 μm) (YMC, Japan). Preparative HPLC was carried out on Waters 1525 HPLC system (Waters, USA). Gas chromatography (GC) analyses were obtained using a Perkin Elmer's Clarus 680 instrument. Melting point testing was carried out on Hanon MP430 melting point apparatus (Hanon Advanced Technology Group Co., Ltd., China).

2.2. Plant Material

The medicinal materials used in this article were provided by Shijiazhuang Yiling Pharmaceutical Co., Ltd., and were identified as the rhizome of *Dryopteris crassirhizoma* Nakai by Tian Qingcun, the director of the company's medicinal materials department, and the specimens of the medicinal materials were stored in Beijing Yiling Pharmaceutical Co., Ltd. The herbarium number of *D. crassirhizoma* is HIB 02230417 (Herbarium of Institute of Botany, Chinese Academy of Sciences)

2.3. Extraction and Isolation

45 kg rhizomes of *D. crassirhizoma* were extracted thrice with 360 liters of water. After extraction, the extracts were combined, concentrated under reduced pressure, and then 95% ethanol was added for alcohol precipitation. The supernatant was vacuum evaporated to obtain the fluid extract. The obtained extract was dispersed with an appropriate amount of water, sequentially extracted with ethyl acetate and n-butanol, and then the ethyl acetate extract (100g), n-butanol extract (328g) and aqueous solution were obtained in order. After the aqueous solution was adsorbed by AB-8 macroporous resin, it was sequentially eluted with water and different concentrations of ethanol (20% ethanol, 40% ethanol, 80% ethanol and 95% ethanol). 20% ethanol eluent was vacuum evaporated to obtain 20% ethanol eluate. This part of the eluate was separated and purified by silica gel column chromatography, sephadex LH-20 column chromatography, MPLC (medium pressure liquid chromatography) with reversed-phase column and pre-HPLC (preparative high performance liquid chromatography) with reversed-phase column to obtain compounds **1** (35 mg), **2** (20 mg), **3** (20 mg), **4** (200 mg), **5** (10 mg), **6** (15 mg), **7** (10 mg), **8** (300 mg), **9** (6 mg), **10** (5 mg) and **11** (38 mg).

2.4. Spectral Data

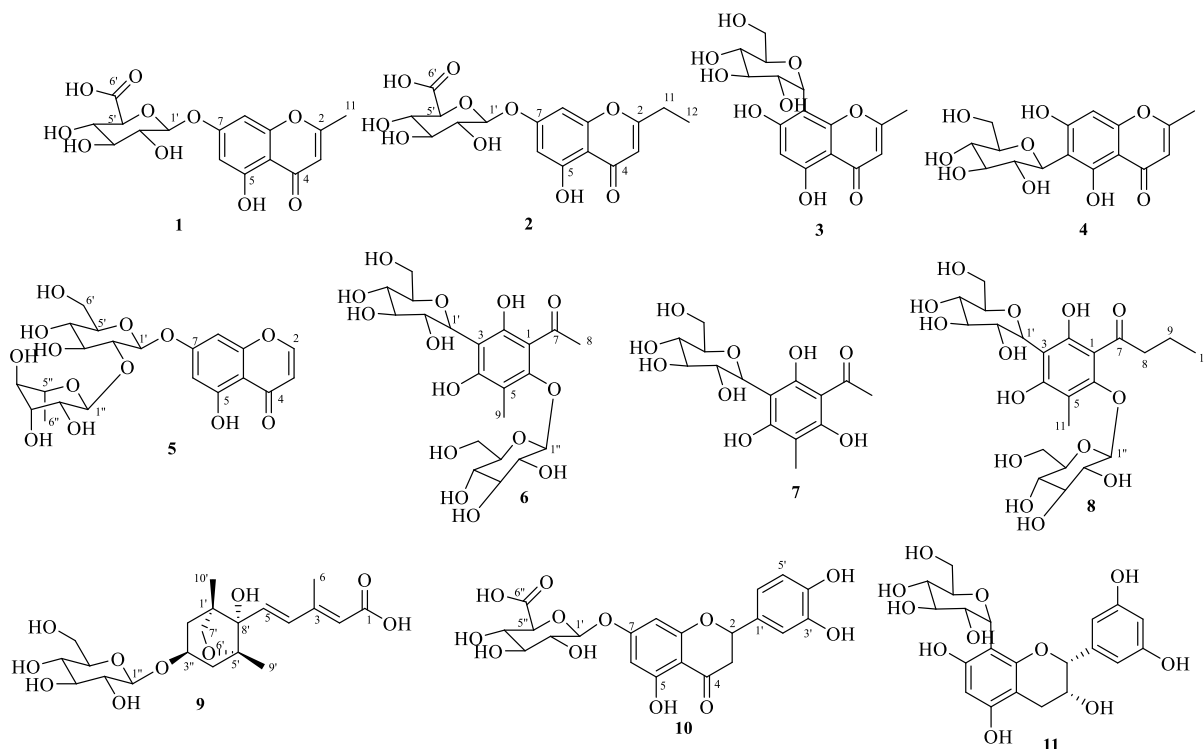
5,7-dihydroxy-2-methylchromone-7-O-β-D-glucuronide (1): Colorless powder; M.P: 158-161°C; IR (KBr) λ_{\max} : 3303, 2907, 1723, 1622, 1502, 1423, 1336, 1259, 1176, 1079, 939, 823, 761, 682, 559 cm^{-1} ; HR-TOF/MS at m/z 369.0814 $[\text{M} + \text{H}]^+$ (calcd for $\text{C}_{16}\text{H}_{16}\text{O}_{10}$, 369.0822); ^1H NMR (600 MHz, $\text{DMSO}-d_6$) and ^{13}C NMR (150 MHz, $\text{DMSO}-d_6$) data (Table 1).

5,7-dihydroxy-2-ethylchromone-7-O-β-D-glucuronide (2): Colorless powder; M.P: Not tested; IR (KBr) λ_{\max} : 3305, 2905, 1720, 1656, 1620, 1502, 1422, 1336, 1260, 1176, 1081, 939, 820, 763, 678, 559 cm^{-1} ; HR-TOF/MS at m/z 383.0971 $[\text{M} + \text{H}]^+$ (calcd for $\text{C}_{17}\text{H}_{18}\text{O}_{10}$, 383.0978); ^1H NMR (600 MHz, $\text{DMSO}-d_6$) and ^{13}C NMR (150 MHz, $\text{DMSO}-d_6$) data (Table 1).

isobiflorin (3): white amorphous powder; M.P: 269-271 °C; ESIMS at m/z 355.1 $[\text{M} + \text{H}]^+$. ^1H NMR ($\text{DMSO}-d_6$, 600 MHz) δ_{H} : 13.00 (1H, s, OH-5), 6.20 (1H, s, H-6), 6.16 (1H, s, H-3), 4.61 (1H, d, $J = 9.6$ Hz, H-1'), 3.86 (1H, br t, $J = 9.0$ Hz, H-2'), 3.67 (1H, d, $J = 10.8$ Hz, H-6'a), 3.40 (1H, dd, $J = 10.8$, 4.8 Hz, H-6'b), 3.20 (1H, t, $J = 7.8$ Hz, H-3'), 3.14-3.16 (2H, m, H₂-4', 5'), 2.33 (3H, s, H₃-11). ^{13}C NMR ($\text{DMSO}-d_6$, 125 MHz) δ_{C} : 182.0 (C-4), 167.2 (C-2), 163.3 (C-7), 160.4 (C-5), 156.4 (C-8a), 107.5 (C-3), 104.5 (C-8), 103.3 (C-4a), 98.6 (C-6), 81.3 (C-5'), 78.6 (C-3'), 73.2 (C-1'), 70.9 (C-2'), 70.5 (C-4'), 61.4 (C-6'), 19.8 (C-11).

biflorin (4): White amorphous powder; M.P: 208-211 °C; M.P: ^1H NMR ($\text{DMSO}-d_6$, 600 MHz) δ_{H} : 13.39 (1H, s, OH-5), 6.34 (1H, s, H-8), 6.15 (1H, s, H-3), 4.55 (1H, d, $J = 10.2$ Hz, H-1'), 4.01 (1H, br t, $J = 9.0$ Hz, H-2'), 3.66 (1H, d, $J = 10.2$ Hz, H-6'a), 3.38 (1H, dd, $J = 10.2$, 6.0 Hz, H-6'b), 3.18-3.09 (3H, m, H-3',4', 5'), 2.34 (3H, s, Me). ^{13}C NMR ($\text{DMSO}-d_6$, 125 MHz) δ_{C} : 182.0 (C-4), 167.3 (C-2), 163.5 (C-7), 160.7 (C-5), 156.7 (C-8a), 108.8 (C-6), 107.8 (C-3), 102.9 (C-4a), 93.4 (C-8), 81.3 (C-5'), 78.9 (C-3'), 73.0 (C-1'), 70.6 (C-2'), 70.1 (C-4'), 61.4 (C-6'), 19.8 (Me).

A new iridoid from the wine-processed corni fructus

**Figure 1.** Chemical structures of compounds **1-11**

5,7-dihydroxychromone-7-O-neohesperidoside (5): M.P: 236-238 °C; White amorphous powder; ^1H NMR (DMSO- d_6 , 600 MHz) δ_{H} : 8.27 (1H, d, $J = 5.4$ Hz, H-2), 6.63 (1H, s, H-8), 6.38 (1H, s, H-6), 6.36 (1H, d, $J = 5.4$ Hz, H-3), 5.20 (1H, d, $J = 7.8$ Hz, H-1'), 5.11 (1H, d, $J = 1.2$ Hz, H-1''), 1.17 (3H, d, $J = 6$ Hz, H-6''). ^{13}C NMR (DMSO- d_6 , 125 MHz) δ_{C} : 181.6 (C-4), 162.6 (C-7), 161.3 (C-5), 158.1 (C-2), 157.4 (C-8a), 110.8 (C-3), 106.6 (C-4a), 100.4 (C-1''), 99.4 (C-6), 97.7 (C-1'), 94.6 (C-8), 77.1, 77.0 (C-3', 5'), 76.1 (C-2'), 71.8 (C-4''), 70.44 (C-3''), 70.36 (C-2''), 69.7 (C-4'), 68.3 (C-5''), 60.5 (C-6'), 18.0 (C-6').

3-C- β -D-glucopyranosyl-5-methylphloroacetophenone-6-O- β -D-glucopyranoside (6): Light yellow powder; M.P: 146-148 °C; IR (KBr) λ_{max} : 3280, 2880, 2103, 1607, 1423, 1361, 1275, 1179, 1128, 1019, 893, 849, 798, 647, 608, 566 cm^{-1} ; HR-TOF/MS at m/z 507.1729 $[\text{M} + \text{H}]^+$ (calcd for $\text{C}_{21}\text{H}_{30}\text{O}_{14}$, 507.1714); ^1H NMR (600 MHz, DMSO- d_6) and ^{13}C NMR (150 MHz, DMSO- d_6) data (Table 1).

3-C- β -D-glucopyranosyl-5-methylphloroacetophenone (7): M.P: 170-172 °C; ^1H NMR (DMSO- d_6 , 600 MHz) δ_{H} : 1.90 (3H, s, H₃-9), 2.58 (3H, s, H₃-8), 3.30 (1H, d, $J = 9.5$ Hz, H-4'), 3.31 (1H, dt, $J = 3.0, 9.5$ Hz, H-5'), 3.35 (1H, t, $J = 9.5$ Hz, H-3'), 3.37 (1H, t, $J = 9.5$ Hz, H-2'), 3.62 (2H, d, $J = 3.0$ Hz, H₂-6'). 4.79 (1H, d, $J = 9.5$ Hz, H-1'), 9.23, 10.70, and 12.58 (each 1H, br s, OH \times 3). ^{13}C NMR (DMSO- d_6 , 125 MHz) δ_{C} : 204.3 (C-7), 163.0 (C-2), 161.6 (C-4), 160.3 (C-6), 106.1 (C-1), 104.3 (C-3), 103.4 (C-5), 33.4 (C-8), and 18.6 (C-9), 81.3 (C-5'), 78.5 (C-3'), 76.2 (C-1'), 73.2 (C-2'), 69.1 (C-4'), 60.4 (C-6').

Dryopteriside (8): Light yellow oil; M.P: 151-153 °C; ESIMS at m/z 535 $[\text{M} + \text{H}]^+$. ^1H NMR (DMSO- d_6 , 600 MHz) δ_{H} : 5.57 (1H, d, $J = 5.4$ Hz, H-1'), 5.09 (1H, d, $J = 4.8$ Hz, H-1''), 2.98-3.11 (2H, m, H-8), 2.10 (3H, s, H-11), 1.58 (2H, m, H-9), 0.88 (3H, t, $J = 7.2$ Hz, H-10). ^{13}C NMR (DMSO- d_6 , 125 MHz) δ_{C} : 207.6 (C-7), 160.2 (C-4), 158.4 (C-2), 155.6 (C-6), 112.5 (C-1), 110.6 (C-5), 109.3 (C-3), 104.6 (C-1''), 81.7 (C-5'), 78.6 (C-3'), 77.3 (C-5''), 76.7 (C-3''), 74.6 (C-1'), 74.6 (C-2''), 72.4 (C-2'), 70.4 (C-4''), 69.8 (C-4'), 61.5 (C-6''), 60.7 (C-6'), 45.6 (C-8), 18.0 (C-10), 14.3 (C-9), 9.6 (C-11).

(2E,4E,1'R,3'S,5'R,8'S)-dihydrophaseic acid 3'-O- β -D-glucopyranoside (9): White amorphous powder; M.P: 206-208 °C; ^1H NMR (DMSO- d_6 , 600 MHz) δ_{H} : 7.90 (1H, d, $J = 15$ Hz, H-4), 6.35 (1H, d, $J = 15$ Hz, H-5), 5.69 (1H, s, H-2), 4.18 (1H, d, $J = 9$ Hz, H-1''), 4.08 (1H, m, H-3'), 3.65 (2H, m, H-7'a, 6'a), 3.56 (1H, d, $J = 6$ Hz, H-7'b), 3.42 (1H, dd, $J = 6$ Hz, 12 Hz, H-6''b), 2.04 (1H, dd, $J = 12, 18$ Hz, H-

2'a), 2.00 (3H, s, H-6), 1.82 (1H, dd, $J = 6, 12$ Hz, H-4'a), 1.63 (2H, m, H-2'b, 4'b), 1.04 (3H, s, H-9'), 0.83 (3H, s, H-10'). ^{13}C NMR (DMSO- d_6 , 125 MHz) δ_{C} : 129.9 (C-4), 101.4 (C-1''), 85.5 (C-5'), 81.2 (C-8'), 76.8 (C-3''), 76.7 (C-5''), 75.1 (C-7'), 73.4 (C-2''), 71.4 (C-3'), 70.1 (C-4''), 61.1 (C-6''), 47.9 (C-1'), 40.1, 39.9 (C-2', 4'), 20.7 (C-6), 19.5 (C-9'), 16.0 (C-10').

R,S-errodityol-7-*O*-glucuronide (**10**): brown powder; M.P: 194-197 °C; ESI-MS m/z : 465 $[\text{M} + \text{H}]^+$. ^1H NMR (DMSO- d_6 , 600 MHz) δ_{H} : 12.05 (1H, s, 5'-OH), 9.09 (1H, s, 4'-OH), 9.04 (1H, s, 3'-OH), 6.90 (1H, $J=1.8$ Hz, H-2'), 6.76 (2H, m, H-5', 6'), 6.19 (1H, d, $J=2.4$ Hz, H-8), 6.15 (1H, d, $J=2.4$ Hz, H-6), 5.46 (1H, dd, $J=12.6, 3.0$ Hz, H-2), 2.74 (1H, m, Ha -3), 3.72 (1H, m, He -3), 5.18 (1H, d, $J=7.2$ Hz, H-1''), 3.98 (1H, m, H-5''). ^{13}C NMR (DMSO- d_6 , 125 MHz) δ_{C} : 79.3 (C-2), 42.7 (C-3), 197.7 (C-4), 103.8 (C-4a), 163.3 (C-5), 96.8 (C-6), 165.2 (C-7), 95.7 (C-8), 163.3 (C-8a), 129.6 (C-1'), 114.9 (C-2'), 145.7 (C-3'), 146.3 (C-4'), 115.8 (C-5'), 118.5 (C-6'), 99.3 (C-1''), 73.2 (C-2''), 76.0 (C-3''), 71.7 (C-4''), 75.7 (C-5''), 170.6 (C-6'').

[2*R*,3*R*]-2,3-*cis*-3,5,7,3',5'-pentahydroxyflavan-8-*C*- α -*D*-glucopyranoside (**11**): light pink powder; M.P: 204-206 °C; ESI-MS m/z : 463 $[\text{M} + \text{H}]^+$. ^1H NMR (DMSO- d_6 , 600 MHz) δ_{H} : 9.07 (1H, s, OH), 8.71 (1H, s, OH), 8.57 (1H, s, OH), 8.18 (1H, s, OH), 4.77 (1H, s, H-2), 3.99 (1H, brs, H-3), 2.47 (1H, m, H-4), 2.67 (1H, m, H-4), 5.92 (1H, s, H-6). ^{13}C NMR (DMSO- d_6 , 125 MHz) δ_{C} : 77.8 (C-2), 65.1 (C-3), 28.5 (C-4), 98.6 (C-4a), 155.2 (C-5), 95.3 (C-6), 155.73 (C-7), 103.9 (C-8), 154.4 (C-8a), 131.2 (C-1'), 114.9 (C-2'), 144.2 (C-3'), 114.5 (C-5'), 117.7 (C-6'), 79.0 (C-1''), 71.9 (C-2''), 74.4 (C-3''), 70.5 (C-4''), 81.2 (C-5''), 61.6 (C-6'').

Table 1. ^1H (600 MHz) and ^{13}C NMR (150 MHz) spectral data of **1**, **2** and **6** in DMSO- d_6

Position	1		2		6	
	δ_{H} , (J in Hz)	δ_{C}	δ_{H} , (J in Hz)	δ_{C}	δ_{H} , (J in Hz)	δ_{C}
1						111.0
2		168.5		173.0		159.4
3	6.25 (s)	108.4	6.23 (s)	107.2		108.2
4		182.1		182.5		161.3
5		161.3		161.6		110.2
6	6.43 (d,1.7)	99.2	6.44 (d,1.5)	99.5		157.5
7		162.5		162.9		204.5
8	6.69 (brs)	94.4	6.71 (brs)	94.8	2.65 (s)	33.2
9		157.5		157.9	2.08 (s)	8.9
10		105.3		105.7		
11	2.39 (s)	20.1	2.68 (q, 7.5)	27.0		
12			1.22 (t, 7.5)	11.1		
2-OH					13.20 (brs)	
4-OH					9.44 (brs)	
5-OH	12.83 (brs)		12.83 (brs)			
1'	5.24 (d,7.4)	99.4	5.25 (d,7.4)	99.8	5.10 (d, 8.9)	75.7
2'	3.28 (m)	72.8	3.28 (m)	73.2	3.53 (m)	71.0
3'	3.30 (m)	75.7	3.30 (m)	76.0	3.26 (m)	77.9
4'	3.38 (t, 9.2)	71.3	3.38 (t, 9.1)	71.7	3.33 (m)	69.2
5'	4.03 (d, 9.7)	75.3	4.02 (d, 9.6)	75.6	3.30 (m)	80.8
6'		170.2		170.6	3.61 (m), 3.64 (brd, 11.1)	59.9
1''					4.69 (d, 7.7)	104.5
2''					3.31 (m)	73.8
3''					3.21 (t, 8.8)	76.2
4''					3.17 (t, 9.1)	69.7
5''					2.99 (m)	76.5
6''					3.46 (m), 3.60 (m)	61.0

2.5. Acid Hydrolysis

A new iridoid from the wine-processed corni fructus

Compounds **1** and **2** were hydrolyzed using 5% HCl to yield the mixture of aglycone and sugar [15]. The sugar in the mixture was further purified by EtOAc extraction to remove the aglycon. After concentration, the sugar was identified by TLC [16] (Merck Silica gel 60 F254) as compared with authentic D-glucuronic acid, the solvent system was EtOAc-MeOH-H₂O-AcOH (10:10:5:0.5) and the developer was 10% sulfuric acid ethanol solution.

Compound **6** (2.0 mg) was separately dissolved in 2% HCl (2 mL) and heated at 70 °C for 12 h. After extraction with EtOAc (3×2 mL) to remove the aglycone, the aqueous layer was evaporated to afford a neutral residue. The dried sugar residue was diluted in anhydrous pyridine (1 mL), to which L-cysteine methyl ester hydrochloride (2 mg) was added. The mixture was stirred at 60 °C for 2 h, and then treated with *N*-trimethylsilylimidazole (0.2 mL). The mixture was then heated to dryness at 60 °C for another 2 h. The dried reactant was partitioned between *n*-hexane (2 mL) and H₂O (2 mL) three times. The *n*-hexane layer was concentrated (1 mL) and subjected to GC analysis (column: Agilent HP-5, 30 m×0.25 mm×0.25 μm, Dikma; detector: FID; detector temperature: 280 °C; injector temperature: 250 °C; carrier: N₂; temperature-programmed: from 200 to 280 °C in 2 min and maintain the final temperature 30 min).

2.6. Molecular Docking

Molecular docking method was used to virtual evaluate the binding affinity between the compound with 3CL hydrolase, a key antiviral target, to provide reference for further experimental verification. AutoDock Vina 1.1.2 is an open-source program for molecular docking and virtual screening. Compared with AutoDock 4, its average accuracy of binding mode prediction is much higher [17]. Compounds of SDF files downloaded from the PubChem database (<https://pubchem.ncbi.nlm.nih.gov/>) [18] and through the Open Babel against 2.4.1 [19] into MOL2 format. The crystal structure of 3CL hydrolase (PDB ID: 7VH8) [20] from novel coronavirus (SARS-CoV-2) was downloaded from PDB database (<https://www.rcsb.org/>) [21]. In addition to the co-crystallized ligand PF-07321332 (nirmatrelvir), we also selected three additional marketed drugs (α -ketoamide, lopinavir, ritonavir) with reported inhibitory effects on 3CL hydrolase as positive controls. Small molecules were energy minimized by using PyRx-0.8 software. Ligands and receptors were prepared according to the AutoDock Vina 1.1.2 tutorial. For each structure, we removed water molecules, added nonpolar hydrogen, calculated Gasteiger charges, and saved them in the PDBQT format. Generally, the lower the Vina score, the higher the Affinity between ligand and receptor. The general selection threshold is binding energy \leq -5 kcal/mol. Finally, Pymol software was used to visualize the interaction mode between compound and 3CL hydrolase.

2.7. Molecular Dynamics Simulation

To dynamically analyze the interaction patterns between receptor 3CL hydrolase and compounds with low molecular docking scores from the kinetic and thermodynamic perspectives, molecular dynamics simulations were performed using GROMACS 4.5 [22]. Protein topological parameters were obtained from CHARMM36 force field [23] by PDB2GMX tool. The electrostatic potential of the inhibitor atom charge was calculated in the Def2-MTZVP base set of ORCA [24], and then the RESP charge was obtained by fitting with the program Multiwfn 3.7 [25]. The complex was placed in a regular dodecahedral TIP3P water box with a side length of 10 Å³, and Na⁺ and Cl⁻ were added to neutralize the system to electroneutrality, followed by energy minimization and pre-balance. Finally, molecular dynamics simulation was performed for 100ns at 300K with a time interval of 2fs, and the energy and coordinate files were saved every 10ps.

3. Results and Discussion

3.1. Structure Elucidation

Compound **1** was obtained as colorless powder. Its molecular formula was deduced to be $C_{16}H_{16}O_{10}$ with HR-TOF/MS at m/z 369.0814 (Calcd 369.0822) $[M+H]^+$. The IR spectrum showed characteristic bands for hydroxyl (3303 cm^{-1}) and carbonyl group (1622 cm^{-1}). The NMR spectra (Table 1) revealed the presence of one anomeric proton at δ_H 5.24 (1H, *d*, $J = 7.4\text{ Hz}$, H-1', with δ_C 99.4), one methyl group at δ_H 2.39 (3H, *s*, H-11, with δ_C 20.1), one hydroxyl proton at δ_H 12.83 (OH, brs, C-5), one olefinic protons at δ_H 6.25 (1H, *s*, H-3, with δ_C 108.4), a pair of meta-coupled aromatic protons at δ_H 6.43 (1H, *d*, $J = 1.7\text{ Hz}$, H-6, with δ_C 99.2) and 6.69 (1H, brs, H-8, with δ_C 94.4). The presence of the aromatic ring fragment and a pair of olefinic fragment were also indicated by the ^{13}C NMR carbon signals at δ_C 161.3 (C-5), 99.2 (C-6), 162.5 (C-7), 94.4 (C-8), 157.5 (C-9), 105.3 (C-10) and δ_C 168.5 (C-2), 108.4 (C-3), respectively. In addition, one ketone carbonyl group at δ_C 182.1 (C-4) and carboxyl carbon at δ_C 170.2 (C-6') were indicated in the ^{13}C NMR spectrum. Combined with the unsaturation analysis, the unsaturations of the compound were nine. Among them, two carbonyl groups were two unsaturations, the glucosyl group was one unsaturation, the benzene ring structure was four unsaturations, and a pair of olefinic protons was one unsaturation, which was still one unsaturation; it was speculated that another cyclic structure existed in the compound structure. The further study on its structure was carried out by 2D NMR spectrum. The HMBC correlations between δ_H 6.25 (H-3) and δ_C 168.5 (C-2) and 182.1 (C-4) suggested that the aglycone of **1** was a type of benzopyran (4-chromone) structure (Figure 2). Acid hydrolysis of **1** yielded D-glucuronic acid, which was identified by TLC. The configurations of the anomeric carbons of the glucosyl fragment was determined to be β by J values at C-1'^[16]. The location of the glucopyranosyl fragment linked to C-7 of the aglycone was determined by the HMBC correlations between δ_H 5.24 (H-1') and δ_C 162.5 (C-7); the location of the methyl fragment linked to C-2 was determined by the HMBC correlation between δ_H 2.39 (H-11) and δ_C 168.5 (C-2), δ_H 2.39 (H-11) and δ_C 108.4 (C-3). The 1H and ^{13}C NMR signals (Table 1) of **1** were completely assigned by a combination of HSQC and HMBC. From these observations, the structure of **1** was identified as 5,7-dihydroxy-2-methylchromone-7-*O*- β -D-glucuronide.

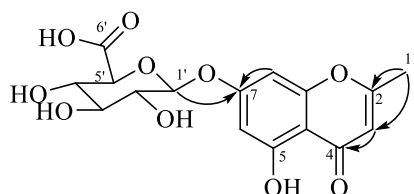


Figure 2. Chemical structure and key HMBC correlations of **1**

Compound **2** was obtained as colorless powder. Its molecular formula was deduced to be $C_{17}H_{18}O_{10}$ with HR-TOF/MS at m/z 383.0971 (Calcd 383.0978) $[M+H]^+$. The IR spectrum showed characteristic bands for hydroxyl (3306 cm^{-1}) and carbonyl group ($1656, 1621\text{ cm}^{-1}$). The NMR spectra (Table 1) revealed the presence of one anomeric proton at δ_H 5.25 (1H, *d*, $J = 7.4\text{ Hz}$, H-1', with δ_C 99.8), one ethyl group at δ_H 2.68 (2H, *q*, $J = 7.5\text{ Hz}$, H-11, with δ_C 27.0) and δ_H 1.22 (3H, *t*, $J = 7.5\text{ Hz}$, H-12, with δ_C 11.1), one hydroxyl proton at δ_H 12.83 (OH, brs, C-5), one olefinic protons at 6.23 (1H, *s*, H-3, with δ_C 107.2), a pair of meta-coupled aromatic protons at δ_H 6.44 (1H, brs, H-6, with δ_C 99.6) and δ_H 6.71 (1H, brs, H-8, with δ_C 94.8). The presence of the aromatic ring fragment and a pair of olefinic fragment were also indicated by the ^{13}C NMR carbon signals at δ_C 161.6 (C-5), 99.5 (C-6), 162.9 (C-7), 94.8 (C-8), 157.9 (C-9), 105.7 (C-10) and δ_C 173.0 (C-2), 107.2 (C-3), respectively. In addition, one ketone carbonyl group at δ_C 182.5 (C-4) and carboxyl carbon at δ_C 170.6, (C-6') were indicated in the ^{13}C NMR spectrum. The NMR data of **2** was similar with that of **1**, except for the substituent group at C-2 of aglycone (Table 1 and Figure 2, 3). In the **2**, the ethyl group linked to C-7 was determined by the HMBC correlation between δ_H 2.68 (H-11) and δ_C 173.0 (C-2), δ_H 1.22 (H-12)

A new iridoid from the wine-processed corni fructus

and δ_C 11.1 (C-11), δ_H 1.22 (H-12) and δ_C 173.0 (C-2). Acid hydrolysis of **2** yielded D-glucuronic acid, which was identified by TLC. The configurations of the anomeric carbons of the glucosyl fragment was determined to be β by J values at C-1'^[16]. The location of the glucopyranosyl fragment linked to C-6 of the aglycone was determined by the HMBC correlations between δ_H 5.25 (H-1') and δ_C 162.9 (C-7). The 1H and ^{13}C NMR signals (Table 1) of **2** were completely assigned by a combination of HSQC and HMBC. From these observations, the structure of **2** was identified as 5,7-dihydroxy-2-ethylchromone-7-*O*- β -D-glucuronide.

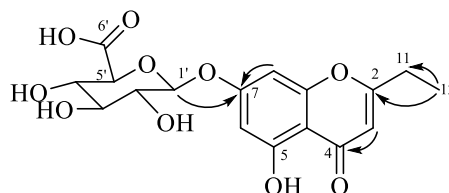


Figure 3. Chemical structure and key HMBC correlations of **2**

Compound **6** was obtained as light-yellow powder. Its molecular formula was deduced to be $C_{21}H_{30}O_{14}$ with HR-TOF/MS at m/z 507.1729 (Calcd 507.1714) $[M+H]^+$. The IR spectrum showed characteristic bands for hydroxyl (3280 cm^{-1}), ketone carbonyl (1608 cm^{-1}) and glycosidic linkage ($1000\text{--}1130\text{ cm}^{-1}$). The ^{13}C NMR spectrum showed 21 carbon signals attributable to an aromatic ring fragment and two hexose residues. The NMR spectra (Table 1) revealed the presence of two anomeric protons at δ_H 4.69 (1H, d , $J = 7.7\text{ Hz}$, H-1' with δ_C 104.5, C-1') and 5.10 (1H, d , $J = 8.9\text{ Hz}$, H-1'' with δ_C 75.7 C-1''), one acetyl groups at δ_H 2.65 (3H, s , H-9 with δ_C 33.2, C-8) and δ_C 204.5 (C-7), one methyl group at δ_H 2.08 (3H, s , H-10 with δ_C 8.9 C-9), and two hydroxyl protons at δ_H 13.20 (OH, brs, C-2) and 9.44 (OH, brs, C-5). The presence of the aromatic ring fragment was indicated by the ^{13}C NMR carbon signals at δ_C 111.0 (C-1), 159.4 (C-2), 108.2 (C-3), 161.3 (C-4), 110.2 (C-5) and 157.5 (C-6). These NMR data indicated that **6** was a phenolic glycoside with two sugar fragments. The absolute configuration of the glucosyl fragments were determined as follow: (1) O-glucosyl fragment: acid hydrolysis of **6** with HCl yielded D-glucose, which was identified by gas chromatograph (GC); the absolute configuration of the O-glucosyl fragment located at C-3 was determined to be D-form; (2) C-glucosyl fragment: by comparing and analyzing C-glucoside NMR data in the literature, the glucose fragment is connected at the C-6 position by carboglycoside bond [26,27]; the absolute configuration of the C-glucosyl fragment located at C-6 was speculated to be D-form, because most of the C-glucosides found in plants were D-form [27]. The configurations of the anomeric carbons of the two glucosyl fragments were determined to be β by J values at C-1' and C'' [16]. The locations of the glucopyranosyl fragments linked to C-3 and C-6 of the aglycone were determined by the HMBC correlation between δ_H 4.69 (H-1') and δ_C 108.2 (C-3), δ_H 5.10 (H-1'') and δ_C 157.5 (C-6); the location of the acetyl fragment linked to C-1 of the aglycone was determined by the HMBC correlations between δ_H 2.65 (H-8) and δ_C 204.5 (C-7), and δ_H 2.65 (H-8) and δ_C 111.0 (C-1). The 1H and ^{13}C NMR signals (Table 1) of **6** were completely assigned by a combination of HSQC and HMBC. From these observations, the structure of **6** was identified as 3-*C*- β -D-glucopyranosyl-5-methylphloracetophenone-6-*O*- β -D-glucopyranoside (Figure 4).

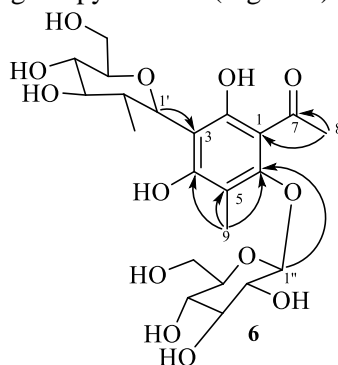


Figure 4. Chemical structure and key HMBC correlations of **6**

3.2. Molecular docking

Based on the key antiviral target 3CL Hydrolase, molecular docking technology was used to evaluate the potential antiviral effect of the 11 candidate compounds obtained in this study (Table 2). In this study, the binding energies of the 11 candidate compounds between 3CL hydrolase targets were all below -5.0 kJ/mol, indicating that these ligands and receptors could bind stably. 5,7-dihydroxychromone-7-*O*-neohesperidoside (**5**) (binding energy = -8.4 kcal/mol) has the same binding free energy as that of 3CL hydrolase co-crystallized molecule PF-07321332. In addition, Luteolin-7-*O*- β -D-glucuronide (**10**) (binding energy = -8.0 kcal/mol) and 3-C- β -D-glucopyranosyl-5-methylphloroacetophenone (**7**) (binding energy = -7.8 kcal/mol) had lower binding free energies with 3CL hydrolase than the other three positive control molecules. The binding free energies between 5,7-dihydroxy-2-methylchromone-7-*O*- β -D-glucuronide (**1**) (binding energy = -7.6 kcal/mol), 5,7-dihydroxy-2-ethylchromone-7-*O*- β -D-glucuronide (**2**) (binding energy = -7.6 kcal/mol), 3-C- β -D-glucopyranosyl-5-methylphloroacetophenone-6-*O*- β -D-glucopyranoside (**6**) (binding energy = -7.5 kcal/mol), and (2E,4E,1'R,3'S,5'R,8'S)-dihydrophaseic acid 3'-*O*- β -D-glucopyranoside (**9**) (binding energy = -7.5 kcal/mol) and 3CL hydrolase were close to the other three positive control molecules. The above results indicated that the candidate compounds could be further studied as potential antiviral compounds. Three novel compounds, the candidate molecule with the lowest binding free energy and the co-crystallized molecule PF-07321332 were selected, and molecular dynamics simulations were carried out subsequently to explore the mechanism of the difference in binding free energy.

3.3. Analysis of Molecular Dynamics Simulation Results

The root mean square deviation (RMSD) of 100 ns time trajectory of molecular dynamics simulation was calculated to test the stability of the system. The results were shown in Figure 5. After the simulation run for 35 ns, the average RMSD of all systems is 0.1~0.3 nm, and the fluctuation range was stable below 0.1 nm, and all of them reached the equilibrium state.

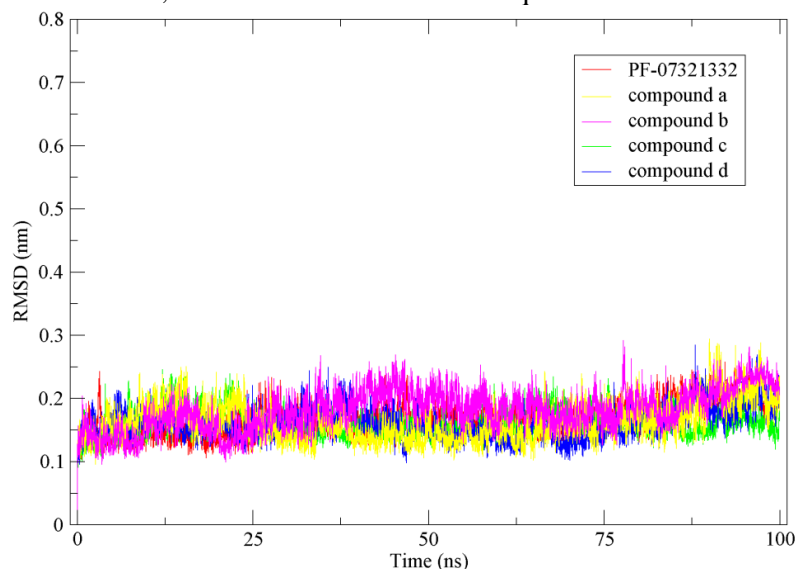


Figure 5. The root mean square deviation (RMSD) of 100 ns time trajectory of molecular dynamics simulation for 3CL hydrolase. **(A)** compound a: 5,7-dihydroxy-2-methylchromone-7-*O*- β -D-glucuronide; **(B)** compound b: 5,7-dihydroxy-2-ethylchromone-7-*O*- β -D-glucuronide; **(C)** compound c: 5,7-dihydroxychromone-7-*O*-neohesperidoside; **(D)** compound d: 3-C- β -D-glucopyranosyl-5-methylphloroacetophenone-6-*O*- β -D-glucopyranoside

A new iridoid from the wine-processed corni fructus

Table 2. Docking scores between compounds with 3CL hydrolase

No.	Compound	Binding energy (kcal /mol)	No.	Compound	Binding energy (kcal /mol)
1	PF-07321332	-8.4	9	5,7-dihydroxychromone-7-O-neohesperidoside (5)	-8.4
2	α -ketoamide	-7.6	10	3-C- β -D-glucopyranosyl-5-methylphloroacetophenone-6-O- β -D-glucopyranoside (6)	-7.5
3	lopinavir	-7.6	11	3-C- β -D-glucopyranosyl-5-methylphloroacetophenone (7)	-7.8
4	ritonavir	-7.5	12	Dryopteriside (8)	-7.4
5	5,7-dihydroxy-2-methylchromone-7-O- β -D-glucuronide (1)	-7.6	13	(2E,4E,1'R,3'S,5'R,8'S)-dihydrophaseic acid 3'-O- β -D-glucopyranoside (9)	-7.5
6	5,7-dihydroxy-2-ethylchromone-7-O- β -D-glucuronide (2)	-7.6	14	Luteolin-7-O- β -D-glucuronide (10)	-8.0
7	Isobiflorin (3)	-7.4	15	[2R,3R]-2,3-cis-3,5,7,3',5'-pentahydroxyflavan-8-C- α -D-glucopyranoside (11)	-7.4
8	Biflorin (4)	-6.8			

Note: Free energy of binding < - 5 kcal/mol is considered to have good binding activity. The lower the binding energy, the more stable is the ligand-receptor binding conformation.

By calculating the root mean square fluctuation (RMSF) of amino acid skeleton atoms in the complex of compound and receptor protein during molecular dynamics simulation, the flexibility of each amino acid residue in protein was analyzed. To evaluate the effect of different small molecule inhibitors on the fluctuation of each amino acid residue of 3C-like proteinase. It was found that the complex formed between four inhibitors and 3C-like proteinase had the similar distribution trends with that of PF-07321332 RMSF values (Figure 6). These results indicated that they could form a stable interaction with the binding pocket of 3CL hydrolase and stabilize the amino acid residues in it.

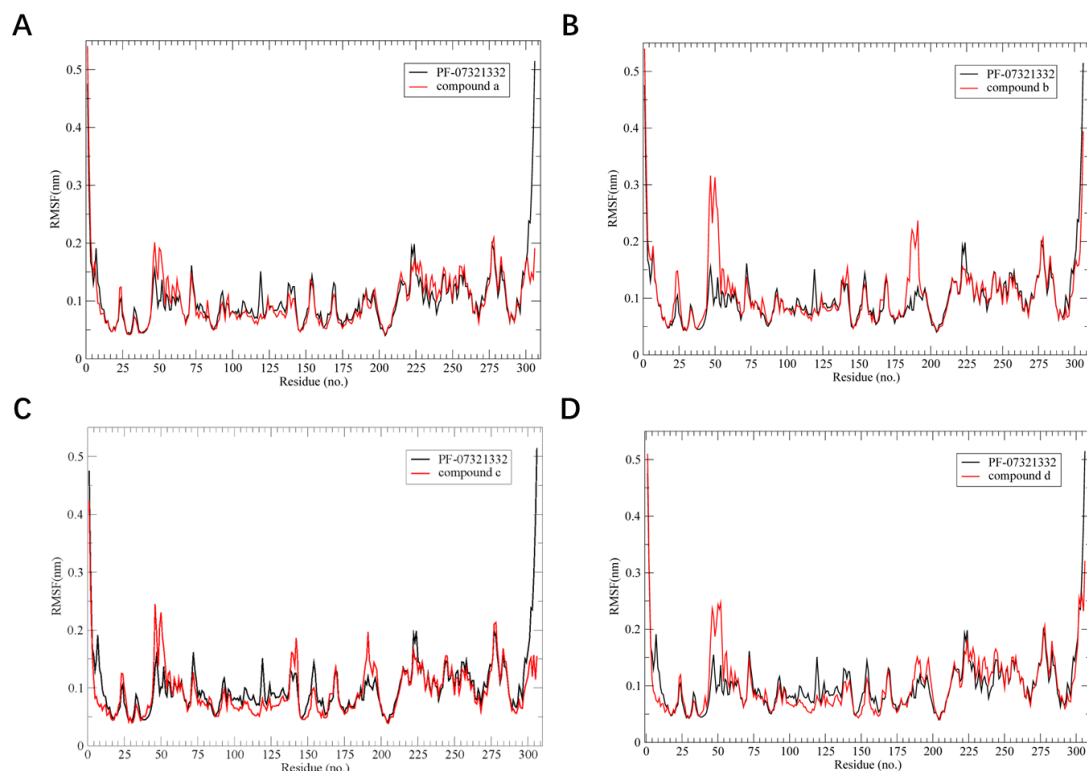


Figure 6. Root mean square fluctuation (RMSF) value fluctuation of amino acid skeleton atom of ligand-protein complex. **(A)** compound a: 5,7-dihydroxy-2-methylchromone-7-O- β -D-glucuronide; **(B)** compound b: 5,7-dihydroxy-2-ethylchromone-7-O- β -D-glucuronide; **(C)** compound c: 5,7-dihydroxychromone-7-O-neohesperidoside; **(D)** compound d: 3-C- β -D-glucopyranosyl-5-methylphloroacetophenone-6-O- β -D-glucopyranoside

3.4. Interaction Mode Between Candidate Compounds and 3CL Hydrolase

We extracted the conformations of the last frame after 100 ns stabilization of the molecular dynamic simulation of the complex between compound and 3CL hydrolase (Figure 7). Hydrogen bonds formed between compounds and amino acid residues are shown in Table 3. As can be seen, the interactions between 3CL hydrolase and co-crystallized molecule PF-07321332 include not only hydrogen bonds, but also C-H bonds, halogen bond interactions and Alkyl interactions. We found that the interaction between compounds and amino acid residues was mainly hydrogen bonds, and 5,7-dihydroxychromone-7-O-neohesperidoside (**5**) formed the largest number of hydrogen bonds with amino acid residues. The hydrogen bond force reduces the binding energy and increases the affinity. The candidate compounds bind closely to the active site of 3CL hydrolase to form a stable complex, which may effectively prevent the attachment of foreign virions and invasion of host cells.

To explore the groups that play key roles in molecules or amino acid residues that play important roles in hydrogen bond formation, we summarized the amino acid residues that form hydrogen bonds with each compound (Table 3). Obviously, the sugar ring structure in the three new compounds (compound **1**, **2** and **6**) plays a key role in the formation of hydrogen bonds compared with the co-crystallized molecule PF-07321332. In addition, the result showed that PF-07321332 forms three hydrogen bonds with the amino acid residues (Asn142, Glu166 and Gln192) of 3CL hydrolase, indicating that these three amino acid residues may be very important in the process of drug action. Glu166 was also involved in hydrogen bond formation during stable conformation of 5,7-dihydroxy-2-methylchromone-7-O- β -D-glucuronide (**1**), 5,7-dihydroxy-2-ethylchromone-7-O- β -D-glucuronide (**2**), and 5,7-dihydroxychromone-7-O-neohesperidoside (**5**) with 3CL hydrolase. Furthermore, we found that two novel amino acid residues, Thr190 and Arg188, play a key role in the formation of four and three new compounds into stable conformations with 3CL hydrolase, suggesting that they may also be of great value in the action of antiviral drugs.

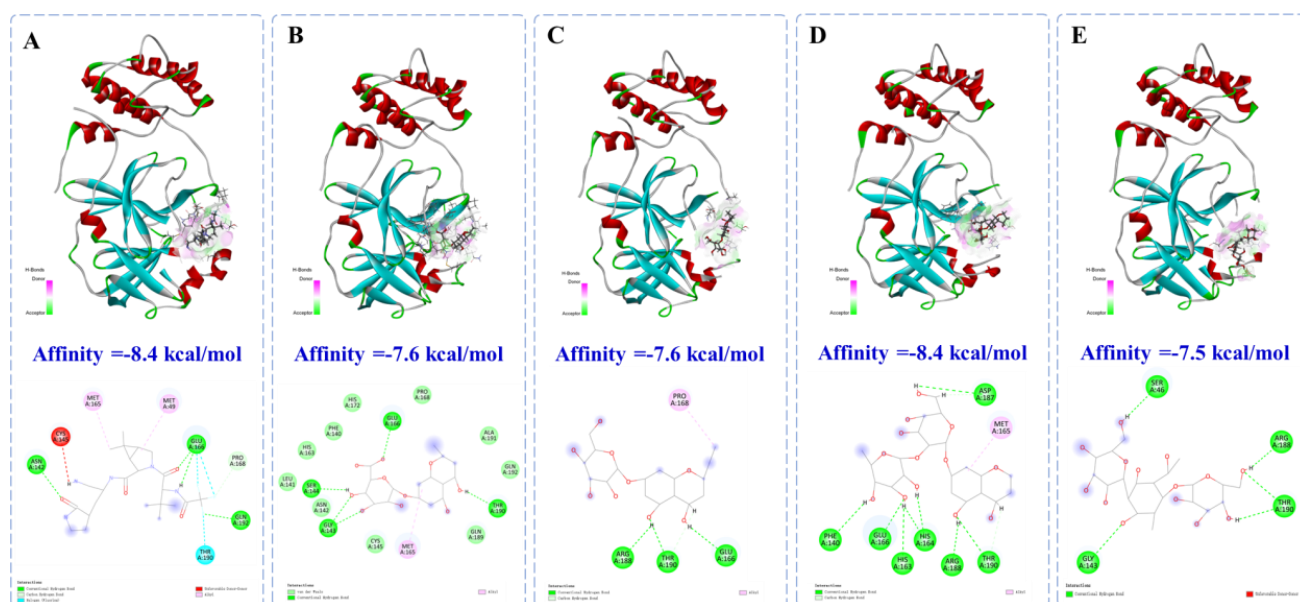


Figure 7. The interaction mode between compounds and 3CL hydrolase. (A) PF-07321332; (B) 5,7-dihydroxy-2-methylchromone-7-O-β-D-glucuronide; (C) 5,7-dihydroxy-2-ethylchromone-7-O-β-D-glucuronide; (D) 5,7-dihydroxychromone-7-O-neohesperidoside; (E) 3-C-β-D-glucopyranosyl-5-methylphloracetophenone-6-O-β-D-glucopyranoside

Since December 2019, there have been repeated outbreaks of the novel coronavirus, and the research and development of effective antiviral drugs remains a hot topic in global medical research. 3CL hydrolase is one of the most critical proteins of coronavirus. 3CL hydrolase of SARS-CoV-2, as a cysteine hydrolase, is one of the major proteases of coronavirus and plays an important role in the process of virus replication. Because its genes are highly conserved, it can be used as a key target for drug design [20,28]. Therefore, searching for SARS-CoV-2 3CL hydrolase inhibitors can provide a more effective way to fight COVID-19. As a Chinese patent medicine with antiviral effect, Lianhua Qingwen capsule has played a positive role in epidemic prevention and control.

In this study, in order to clarify the constituents of *D. crassirhizoma* in LHQW capsule, we used the same preparation process as LHQW capsule to prepare the water extract of *D. crassirhizoma*, from which 11 compounds were separated, mainly flavonoids. This is different from the research on the constituents extracted by ethanol in the literature. The components extracted by ethanol are mainly phloroglucinols with small polarity.

Molecular docking refers to the use of computer simulation combining ligand and receptor proteins, and then to predict a combination of both physical and chemical parameters by calculation model and affinity, it as a combination of physical and chemical principles and scientific computing algorithm of emerging research methods, to explore Chinese medicine medicinal material base and mechanism provides a feasible strategy, promote the modernization of Chinese medicine [29-31]. At present, it is widely used in the discovery of active compounds in traditional Chinese medicine [28,32]. In this study, we systematically evaluated the antiviral potential of 11 compounds (including three compounds with novel structures) by using virtual molecular docking method based on 3CL hydrolase.

Table 3. Interaction of hydrogen bond formed between compound and 3CL hydrolase

#	Compound Name	H-Bond Residues	Van der Waals Residues	C-H Bond Residues	Halogen Residues	Alkyl Residues	unfavorable donor-donor Residues
1	PF-07321332	Asn142, Glu166, Gln192	-	Pro168	Glu166, Thr190	Met165, Met49	Cys145
2	5,7-dihydroxy-2-methylchromone-7- <i>O</i> - β -D-glucuronide	Ser144, Gly143, Glu166, Thr190	Ala191, Asn142 , Cys145 , Gln189, Gln192, His163, His172, Leu141 , Pro168	-	-	Met165	-
3	5,7-dihydroxy-2-ethylchromone-7- <i>O</i> - β -D-glucuronide	Arg188, Thr190, Glu166	-	Thr190	-	-	Pro168
4	5,7-dihydroxychromone-7- <i>O</i> -neohesperidoside	Phe140, Glu166, His163, His164, Arg188, Thr190, Asp187	-	Asp168, Thr190	-	-	Met165
5	3-C- β -D-glucopyranosyl-5-methylphloroacetophenone-6- <i>O</i> - β -D-glucopyranoside	Gly143, Ser46, Arg188, Thr190	-	-	-	-	-

The co-crystallized ligand PF-07321332 (nirmatrelvir) was selected as the positive control molecule. To improve data reliability, three additional marketed drugs (α -ketoamide, lopinavir, ritonavir) with reported inhibitory effects on 3CL hydrolase as positive controls. Nirmatrelvir and ritonavir are components of Paxlovid, the first oral COVID-19 drug in the United States, made by Pfizer. Based on the molecular docking results of 11 compounds and positive control molecules, 5,7-dihydroxychromone-7-*O*-neohesperidoside (**5**) (binding energy = -8.4 kcal/mol), Luteolin-7-*O*- β -D-glucuronide (**10**) (binding energy = -8.0 kcal/mol), 3-C- β -D-glucopyranosyl-5-methylphloroacetophenone (**7**) (binding energy = -7.8 kcal/mol), 5,7-dihydroxy-2-methylchromone-7-*O*- β -D-glucuronide (**1**) (binding energy = -7.6 kcal/mol), 5,7-dihydroxy-2-ethylchromone-7-*O*- β -D-glucuronide (**2**) (binding energy = -7.6 kcal/mol), 3-C- β -D-glucopyranosyl-5-methylphloroacetophenone-6-*O*- β -D-glucopyranoside (**6**) (binding energy = -7.5 kcal/mol), and

A new iridoid from the wine-processed corni fructus

(2E,4E,1' R,3' S,5' R,8' S)-dihydrophaseic acid 3' -O- β -D-glucopyranoside (**9**) (binding energy = -7.5 kcal/mol) can be preferentially selected for experimental verification in subsequent studies. In addition, molecular dynamics simulation using GROMACS software can not only show the interaction details of protein and inhibitor at the atomic and molecular levels, but also facilitate the elucidated structural affinity relationship between protein and inhibitor complex. Molecular dynamics simulation showed that the structure of sugar ring in the new structure compounds played an important role in hydrogen bond formation. In addition, two new amino acid residues, Thr190 and Arg188, were found to be potential important residues for antiviral drugs to form stable conformations with 3CL hydrolase.

4. Conclusion

In this study, a total of 11 compounds were obtained from the composition of *D. crassirhizoma* in Lianhua Qingwen capsule, among which 3 were novel: 5,7-dihydroxy-2-methylchromone-7-O- β -D-glucuronide (**1**), 5,7-dihydroxy-2-ethylchromone-7-O- β -D-glucuronide (**2**), 3-C- β -D-glucopyranosyl-5-methylphloracetophenone-6-O- β -D-glucopyranoside (**6**). On this basis, we conducted an exploratory study on the antiviral potential of these 11 compounds based on the 3CL hydrolase, which plays a key role in the replication of SARS-CoV-2 virus. The results of molecular virtual docking indicated that most of the compounds had antiviral potential. Molecular dynamics simulation showed that the new structure compounds could form a stable complex with 3CL hydrolase, and the structure of sugar ring in the compound played an important role in hydrogen bond formation. The stability of the complex was comparable to that of the anti-COVID-19 drugs currently on the market, and it had important potential against COVID-19. In addition, two new amino acid residues, Thr190 and Arg188, were found to be potential important residues for antiviral drugs to form stable conformations with 3CL hydrolase and thus play a therapeutic role. The new findings of this study can provide some new perspectives and references for the design of antiviral drugs, and also provide a research paradigm for identifying active substances from TCM compounds with antiviral activity in clinical application.

Acknowledgments

We gratefully acknowledge financial support from the National Natural Science Foundation of China (82130123). We also wish to extend our thanks to any individual for their assistance in the conduction of this study.

Supporting Information

Supporting information accompanies this paper on <http://www.acgpubs.org/journal/records-of-natural-products>

ORCID

Yunbo Sun: [0000-0002-1076-8457](https://orcid.org/0000-0002-1076-8457)

Tongxing Wang: [0000-0002-4008-7230](https://orcid.org/0000-0002-4008-7230)

Shuo Shen: [0000-0002-0470-2638](https://orcid.org/0000-0002-0470-2638)

Dan Bi: [0000-0001-7402-3270](https://orcid.org/0000-0001-7402-3270)

Fengjun He: [0000-0002-7540-0805](https://orcid.org/0000-0002-7540-0805)

Bin Hou: [0000-0001-5350-5027](https://orcid.org/0000-0001-5350-5027)

Yifu Zhang: [0000-0001-6548-9220](https://orcid.org/0000-0001-6548-9220)

Ya Tian: [0000-0001-6366-7775](https://orcid.org/0000-0001-6366-7775)

Chuangfeng Zhang: [0000-0002-8274-0154](https://orcid.org/0000-0002-8274-0154)

Zhenhua Jia: [0000-0001-5132-1099](https://orcid.org/0000-0001-5132-1099)

References

- [1] F. Qi and E. Wang (2007). Studies on active constituents in rhizome of *Dryopteris crassirhizoma*, *J. Tianjing Medical Univ.* **2**, 191-193.
- [2] L.P. Yuan, G.T. Deng, X.Z. Jia, H.Y. Liu, X.H. Yang and Z.B. Shen (2016). Study on the chemical constituents of petroleum ether extract fraction from *Dryopteris crassirhizoma* Nakai, *J. Guangdong Pharmaceut. Univ.* **32**, 19-21.
- [3] Y. Yang, G.J. Lee, D.H. Yoon, T. Yu, J. Oh, D. Jeong, J. Lee, S.H. Kim, T.W. Kim and J.Y. Cho (2013). ERK1- and TBK1-targeted anti-inflammatory activity of an ethanol extract of *Dryopteris crassirhizoma*, *J. Ethnopharmacol.* **145**, 499-508.
- [4] S.H. Chang, J.H. Bae, D.P. Hong, K.D. Choi, S.C. Kim, E. Her, S.H. Kim and C.D. Kang (2010). *Dryopteris crassirhizoma* has anti-cancer effects through both extrinsic and intrinsic apoptotic pathways and G0/G1 phase arrest in human prostate cancer cells, *J. Ethnopharmacol.* **130**, 248-254.
- [5] S.M. Lee, M.K. Na, R.B. An, B.S. Min and H.K. Lee (2003). Antioxidant activity of two phloroglucinol derivatives from *Dryopteris crassirhizoma*, *Biol. Pharm. Bull.* **26**, 1354-1356.
- [6] B.S. Min, M. Tomiyama, C.M. Ma, N. Nakamura and M. Hattori (2001). Kaempferol acetylramnosides from the rhizome of *Dryopteris crassirhizoma* and their inhibitory effects on three different activities of human immunodeficiency virus-1 reverse transcriptase. *Chem. Pharm. Bull.* **49**, 546-550.
- [7] J. Wang, Y.T. Yan, S.Z. Fu, B. Peng, L.L. Bao, Y.L. Zhang, J.H. Hu, Z.P. Zeng, D.H. Geng and Z.P. Gao (2017). Anti-influenza virus (H5N1) activity screening on the phloroglucinols from Rhizomes of *Dryopteris crassirhizoma*, *Molecules.* **22**, doi: 10.3390/molecules22030431.
- [8] Y. Jia, J. Zhao, X. Han and S. Li (2017). Research progress on chemical composition and pharmacological activities of *Dryopteridis Crassirhizomatis* rhizome, *Asia-Pacific Trad. Medic.*, **13**, 53-56.
- [9] G.L. Yang, Y. Zhang, C.H. Nan, K.F. Sun, Y.L. Xu and K.M. Zhao (2010). Study on inhibitory effect of five kinds of traditional Chinese medicine including *Dryopteris Crassirhizoma* on influenza A virus FM1 strain, *J. Pract. Trad. Chin. Inter. Medic.* **24**, 3-4.
- [10] Y.T. Yan, J. Wang, D.H. Geng, S.Z. Fu, J.H. Hu and Z.P. Gao (2018). Screening of active components from phloroglucinols in Mianma Guanzhong for anti-neuraminidase of H1N1 influenza virus, *J. Beijing Univ. Trad. Chin. e Medic.* **41**, 71-75.
- [11] J.S. Lee, H. Miyashiro, N. Nakamura and M. Hattori (2008). Two new triterpenes from the rhizome of *Dryopteris crassirhizoma*, and inhibitory activities of its constituents on human immunodeficiency virus-1 protease, *Chem. Pharm. Bull.* **56**, 711-714.
- [12] Z. Jin, X. Du, Y. Xu, Y. Deng, M. Liu, Y. Zhao, B. Zhang, X. Li, L. Zhang and C. Peng (2020). Structure of M(pro) from SARS-CoV-2 and discovery of its inhibitors, *Nature* **582**, 289-293.
- [13] P. Zhou, X.L. Yang, X.G. Wang, B. Hu, L. Zhang, W. Zhang, H.R. Si, Y. Zhu, B. Li and C.L. Huang (2020). A pneumonia outbreak associated with a new coronavirus of probable bat origin, *Nature* **579**, 270-273.
- [14] Y.R. Liu, Z.S. Tang, M. Wang, J.A. Duan, Z.X. Song, R. Zhou, Z. Wang, H. Li, X.H. Li and D.H. Jiang (2020). Potential SARS-CoV-2 3CL protease inhibitors selection from TCMSF platform, *Chin. Tradit. Herbal Drug.* **51**, 1694-1703.
- [15] K. Kamiya, Y. Saiki, T. Hama, Y. Fujimoto, H. Endang, M. Umar and T. Satake (2001). Flavonoid glucuronides from *Helicteres isora*, *Phytochemistry* **57**, 297-301.
- [16] B. Ryu, H.M. Kim, J.S. Lee, C.K. Lee, J. Sezirahiga, J.H. Woo, J.H. Choi and D.S. Jang (2016). New flavonol glucuronides from the flower buds of *Syzygium aromaticum* (Clove), *J. Agric. Food Chem.* **64**, 3048-3053.
- [17] O. Trott and A.J. Olson (2010). AutoDock Vina: improving the speed and accuracy of docking with a new scoring function, efficient optimization, and multithreading, *J. Comput. Chem.* **31**, 455-461.
- [18] S. Kim, P.A. Thiessen, E.E. Bolton, J. Chen, G. Fu, A. Gindulyte, L. Han, J. He, S. He and B.A. Shoemaker (2016). PubChem Substance and Compound databases, *Nucleic Acid. Res.* **44**, D1202-1213.
- [19] N.M. O'Boyle, M. Banck, C.A. James, C. Morley, T. Vandermeersch and G.R. Hutchison (2011). Open Babel: An open chemical toolbox, *J. Cheminform.* **3**, 33.
- [20] Y. Zhao, C. Fang, Q. Zhang, R. Zhang, X. Zhao, Y. Duan, H. Wang, Y. Zhu, L. Feng and J. Zhao (2022). Crystal structure of SARS-CoV-2 main protease in complex with protease inhibitor PF-07321332, *Protein. Cell* **13**, 689-693.
- [21] M.P. Karuppasamy, S. Venkateswaran and P. Subbiah (2020). PDB-2-PBv3.0: An updated protein block database. *J. Bioinf. Comput. Biol.* **18**, 2050009, doi: 10.1142/S0219720020500092.

A new iridoid from the wine-processed corni fructus

- [22] M.J. Abraham, T. Murtola, R. Schulz, S. Páll, J.C. Smith, B. Hess and E. Lindahl (2015). GROMACS: High performance molecular simulations through multi-level parallelism from laptops to supercomputers, *SoftwareX*, **1**, 19-25.
- [23] J. Huang and A.D.Jr. MacKerell (2013). CHARMM36 all-atom additive protein force field: validation based on comparison to NMR data, *J. Comput. Chem.* **34**, 2135-2145.
- [24] F. Neese (2011). The ORCA program system, *WIREs Comput. Mol. Sci.* **2**, 73-78.
- [25] T. Lu and F. Chen (2012). Multiwfn: a multifunctional wavefunction analyzer, *J. Comput. Chem.* **33**, 580-592.
- [26] Y.W. Zhang. and Y.W. Cao. (1997). Isobiflorin a chromone C-glucoside from cloves (*Eugenia caryophyllata*). *Phytochemistry* **45**, 401-403.
- [27] X. Chang, W. Li, K. Koike, L. Wu and T. Nikaido (2006). Phenolic constituents from the rhizomes of *Dryopteris crassirhizoma*, *Chem. Pharm. Bull.* **54**, 748-750.
- [28] K.M. Santiago-Silva, P. Camargo, G. Felix da Silva Gomes, A.P. Sotero, A. Orsato, C.C. Perez, G. Nakazato, C.H. da Silva Lima and M. Bispo (2022). In silico approach identified benzoylguanidines as SARS-CoV-2 main protease (M(pro)) potential inhibitors, *J. Biomol. Struct. Dyn.* doi: 10.1080/07391102.2022.2123396.
- [29] I. Nawrot-Hadzik, M. Zmudzinski, A. Matkowski, R. Preissner, M. Kęsık-Brodacka, J. Hadzik, M. Drag and R. Abel (2021). *Reynoutria* rhizomes as a natural source of SARS-CoV-2 Mpro inhibitors-molecular docking and in vitro study, *Pharmaceuticals (Basel)*, **14**, doi: 10.3390/ph14080742.
- [30] S. Mohandoss, R. Sukanya, S. Ganesan, F.H. Alkallas, A. Ben Gouider Trabelsi, F.V. Kusmartsev, K. Sakthi Velu, T. Stalin, H.M. Lo and Y. Rok Lee (2022). SARS-CoV-2 main protease (3CL(pro)) interaction with acyclovir antiviral drug/methyl- β -cyclodextrin complex: Physiochemical characterization and molecular docking, *J. Mol. Liq.*, **366**, doi: 10.1016/j.molliq.2022.120292.
- [31] P.M. Wadanambi, N. Jayathilaka and K.N. Seneviratne (2022). A computational study of carbazole alkaloids from *Murraya koenigii* as potential SARS-CoV-2 main protease inhibitors, *Appl. Biochem. Biotechnol.* **195**, 573-596.
- [32] W.S. Qayed, R.S. Ferreira and J.R.A. Silva (2022). In silico study towards repositioning of FDA-approved drug candidates for anticoronaviral therapy: molecular docking, molecular dynamics and binding free energy calculations, *Molecules* **27**, Article ID:5988, doi: 10.3390/molecules27185988.

A C G
publications

© 2023 ACG Publications